

Supplementary Materials

Loss of *LBP* triggers lipid metabolic disorder through H3K27 acetylation-mediated *C/EBPβ-SCD* activation in non-alcoholic fatty liver disease

Ya-Ling Zhu ^{1,2,#}, Lei-Lei Meng ^{1,#}, Jin-Hu Ma ^{1,#}, Xin Yuan ¹, Shu-Wen Chen ¹, Xin-Rui Yi ¹, Xin-Yu Li ¹, Yi Wang ¹, Yun-Shu Tang ^{1,2}, Min Xue ¹, Mei-Zi Zhu ¹, Jin Peng ¹, Xue-Jin Lu ¹, Jian-Zhen Huang ⁴, Zi-Chen Song ¹, Chong Wu ¹, Ke-Zhong Zheng ³, Qing-Qing Dai ³, Fan Huang ^{3,*}, Hao-Shu Fang ^{1,2,*}

¹ *Department of Pathophysiology, Anhui Medical University, Hefei, Anhui 230032, China*

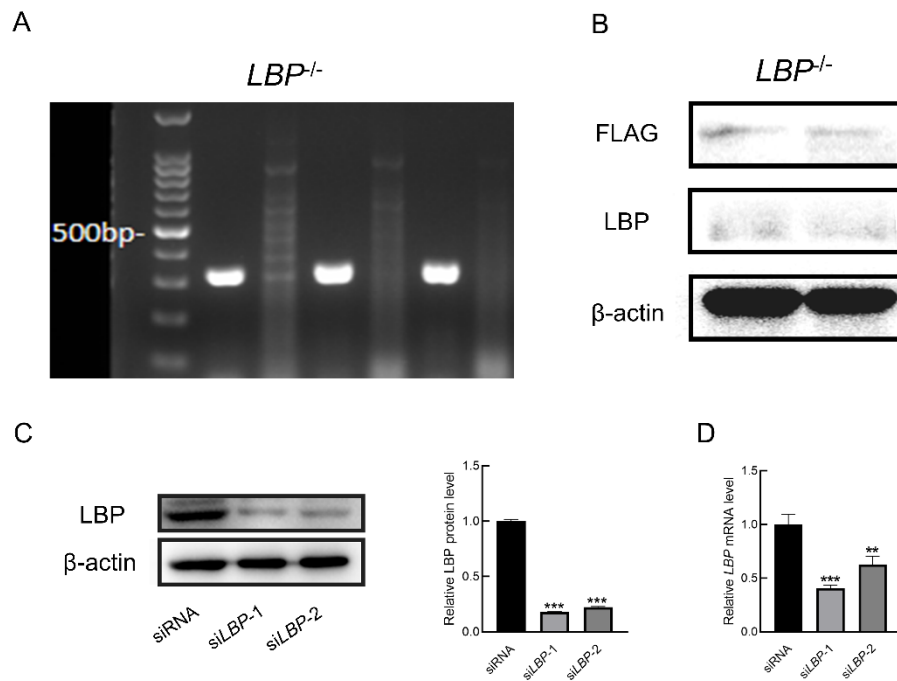
² *Laboratory Animal Research Center, School of Basic Medical Sciences, Anhui Medical University, Hefei, Anhui 230032, China*

³ *Department of Hepatobiliary Surgery, First Affiliated Hospital of Anhui Medical University, Hefei, Anhui 230022, China*

⁴ *College of Animal Science and Technology, Jiangxi Agricultural University, Nanchang, Jiangxi 330045, China*

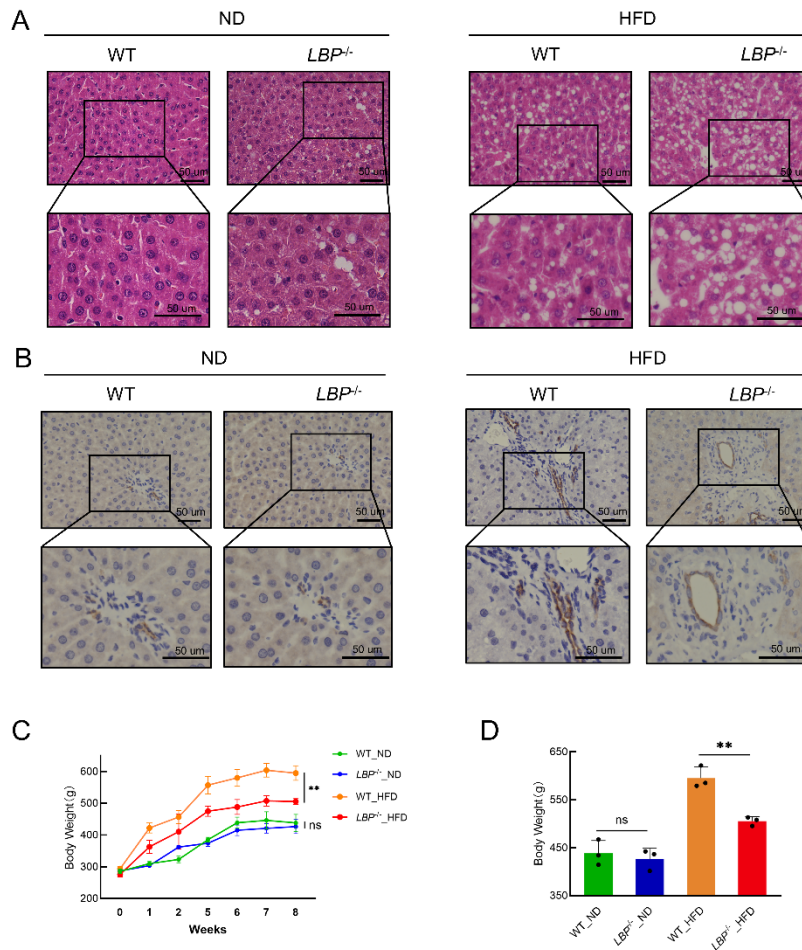
#Authors contributed equally to this work

*Corresponding authors, E-mail: huang_f@vip.126.com; fanghaoshu@ahmu.edu.cn



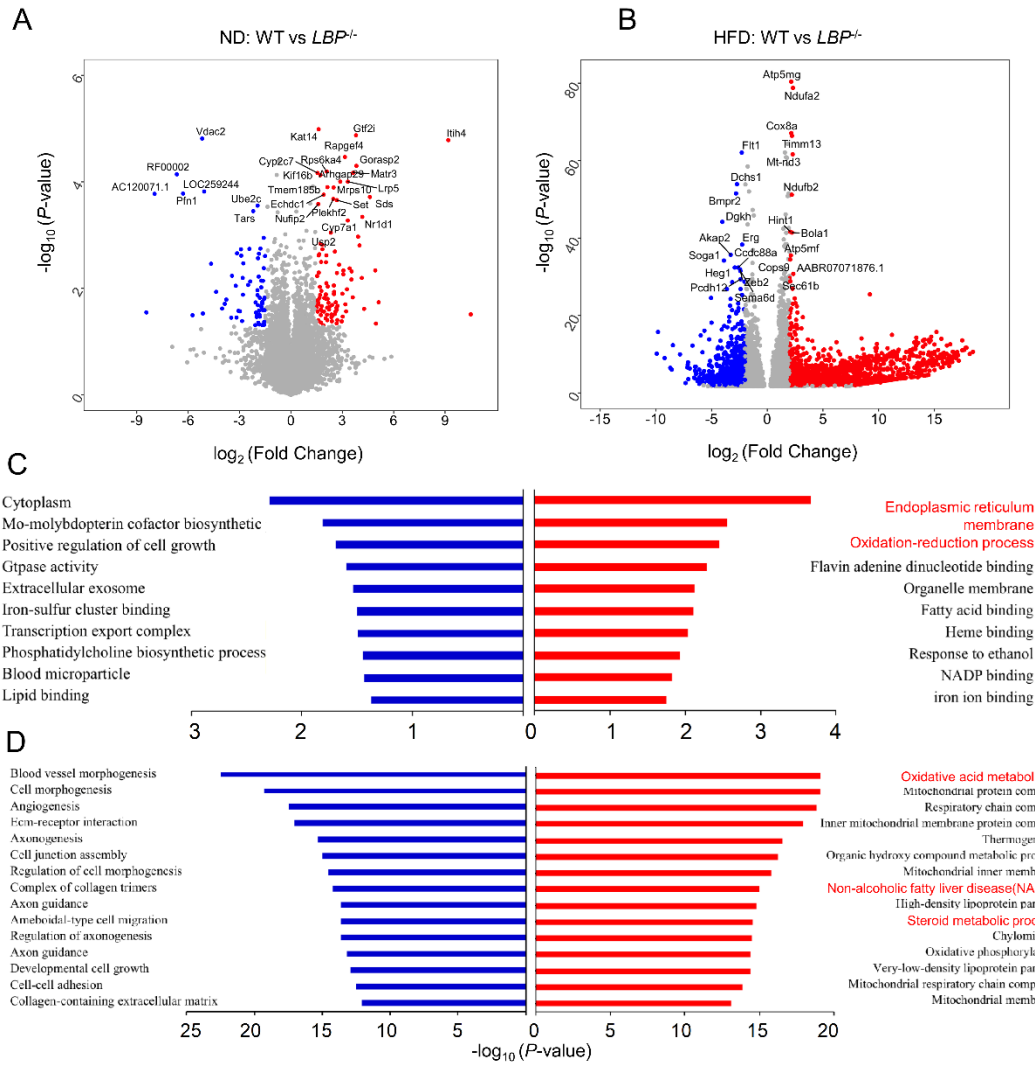
Supplementary Figure S1 Validation of efficiency of *LBP* knockout *in vivo* and *LBP* knockdown *in vitro*

A–B: Agarose electrophoresis (A) and western blot (B) analysis showing significantly decreased RNA and protein concentrations after *LBP* deficiency treatment, respectively. C, D: Western blot (C) and RT-qPCR (D) analysis of *LBP* expression in BRL-3A hepatocytes transfected with siRNA or si*LBP* ($n=3$ /group). Student's *t*-test was performed for data analysis. **: $P<0.01$, ***: $P<0.001$. Data are shown as mean \pm SD.



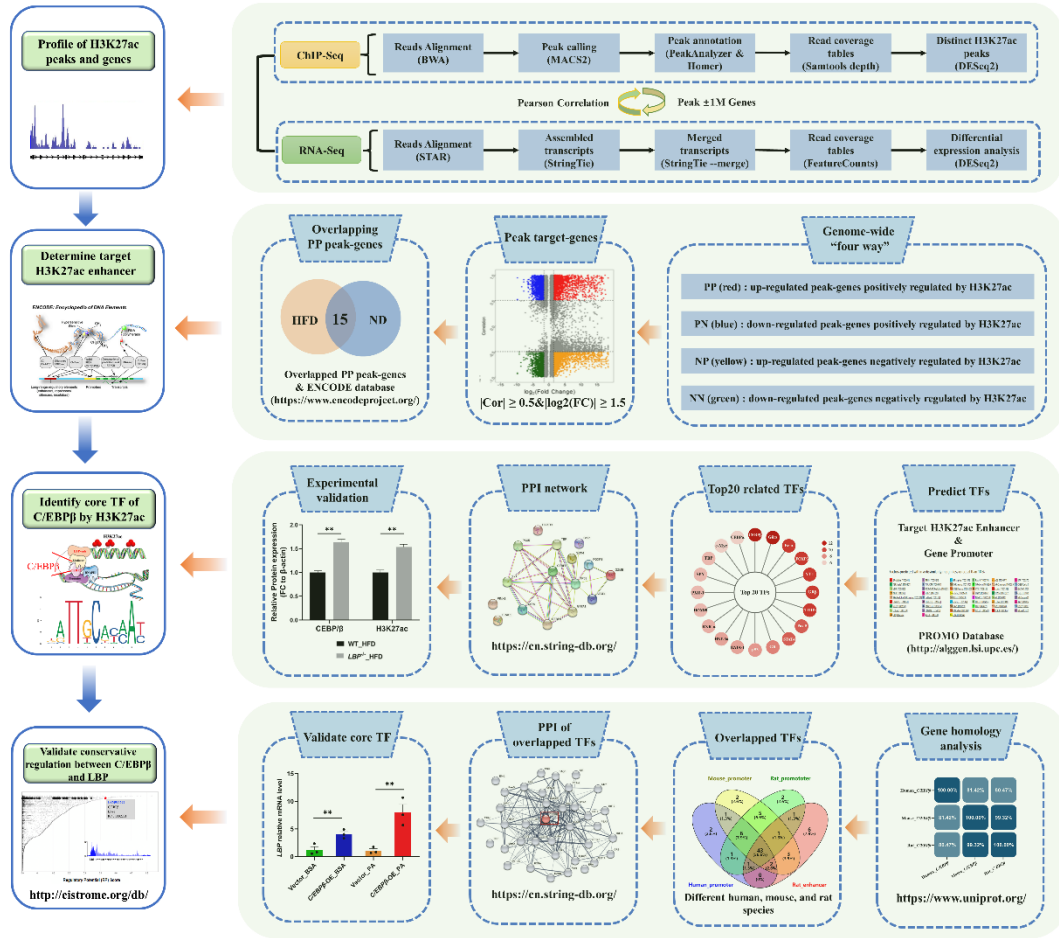
Supplementary Figure S2 Liver lipid accumulation and inflammation and body weight changes induced by *LBP* deficiency

A: Enlargement of H&E-stained liver sections in Figure 1C showing aggravated lipid accumulation induced by *LBP* deficiency and HFD feeding (scale bar, 50 μ m), $n=6$ /group. B: Representative immunohistochemical staining for Inducible nitric oxide synthase (iNOS) of liver tissues in indicated groups (scale bar, 50 μ m), $n=6$ /group. C: Body weight change during 8 weeks in WT and *LBP*^{-/-} rats fed with ND and HFD. D: Body weight at time of harvest. $n=3$ /group. One-way ANOVA was performed for data analysis. ns: Not significant; **: $P<0.01$. All data are shown as mean \pm SD.

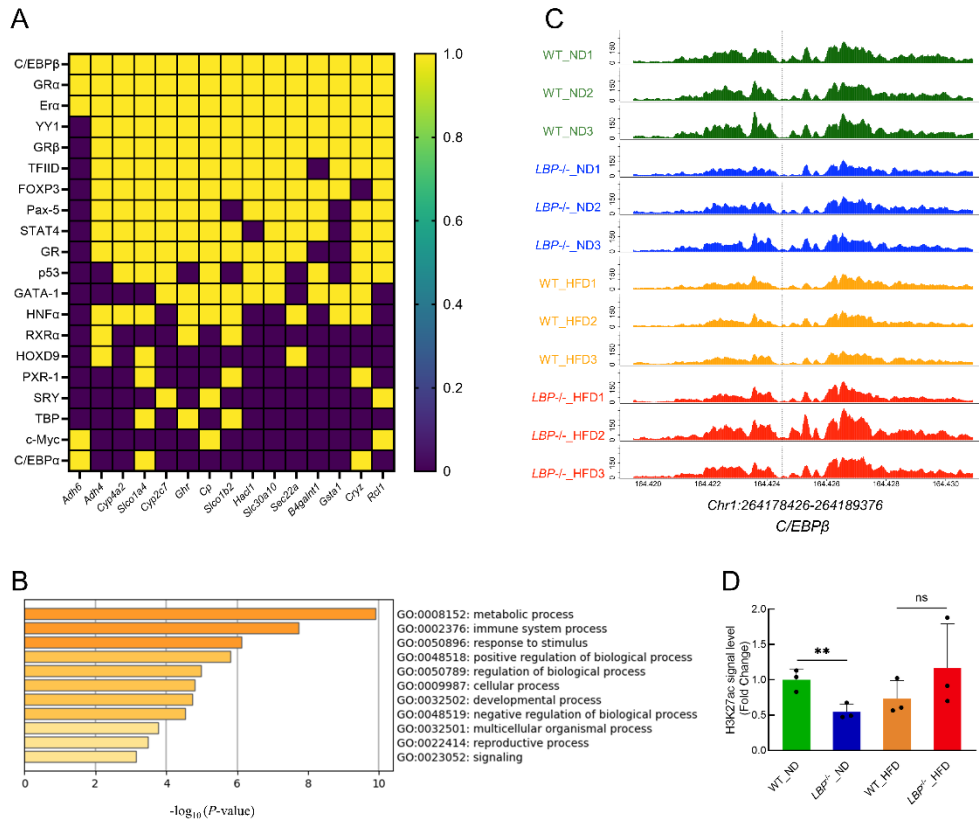


Supplementary Figure S3 *LBP* deficiency aggravates lipid metabolism disorders induced by HFD

A, B: Volcano plots showing significant differentially expressed genes (DEGs) between *LBP*^{-/-} and WT rats fed with ND (A) or HFD (B). Red, blue, and gray indicate up-regulated, down-regulated, and unchanged, respectively. C, D: Regulatory terms of markedly up-regulated (red) and down-regulated DEGs (blue) in liver from *LBP*^{-/-} and WT rats fed with ND (C) and HFD (D) by DAVID (<https://david-d.ncifcrf.gov/>) (ranked by corrected *P*-values).

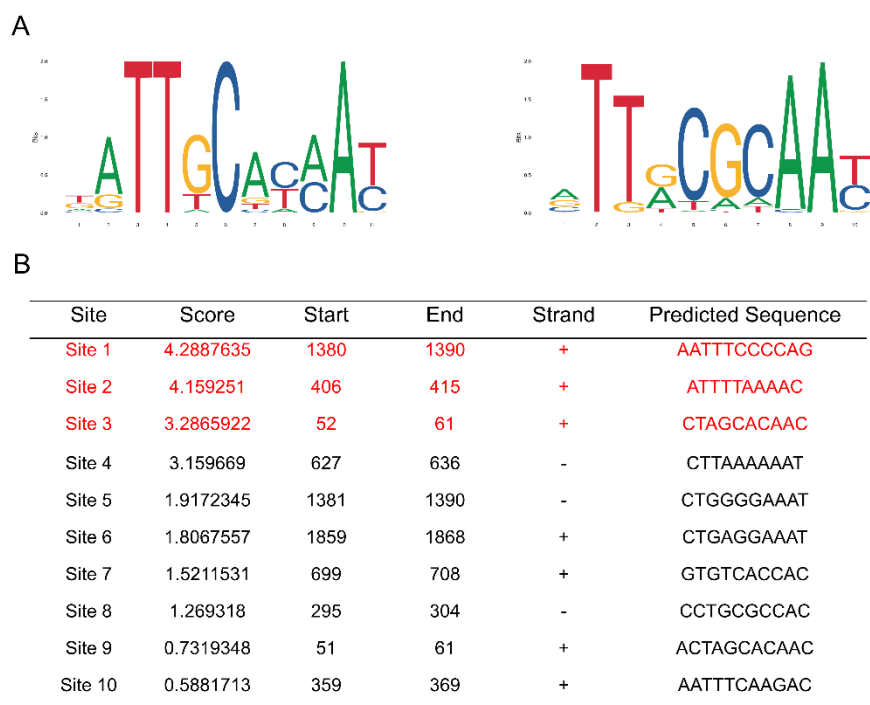


Supplementary Figure S4 Study workflow of core transcription identification



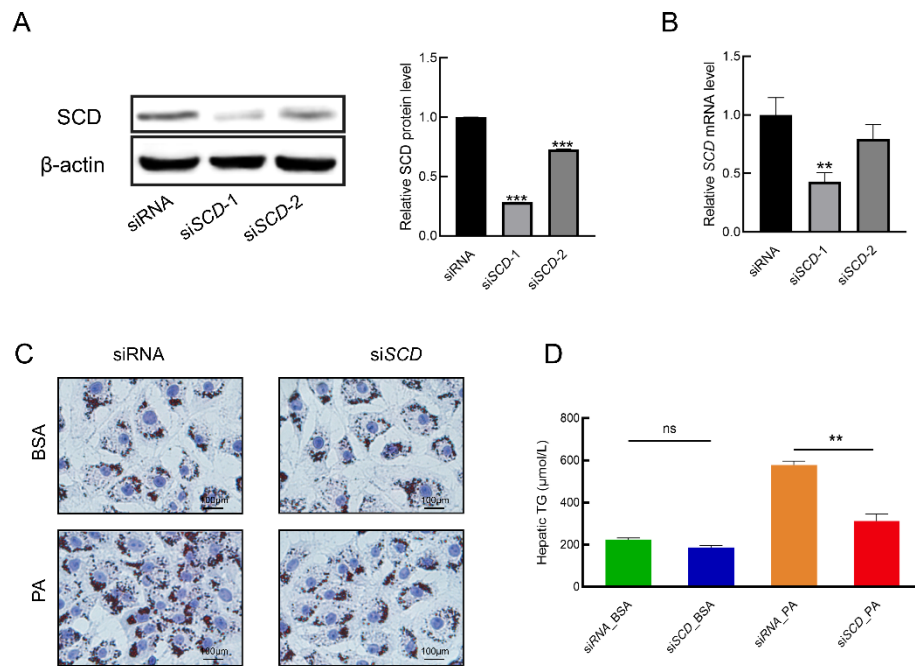
Supplementary Figure S5 C/EBPβ may act as a critical mediator during development of NAFLD with LBP deficiency

A: Heatmap showing regulatory relationship between 15 overlapping PP peak-genes and top 20 predicted TFs. B: GO enrichment analysis of top 20 TFs by Metascape (<https://metascape.org/gp/>). C, D: Genome browser representation (C) and quantification (D) showing activity of *Chr1:264178426-264189376*, which tracks at *C/EBPβ* locus in indicated individuals ($n=3$ /group). One-way ANOVA was performed for data analysis. ns: Not significant; **: $P < 0.01$. Data are shown as mean \pm SD.



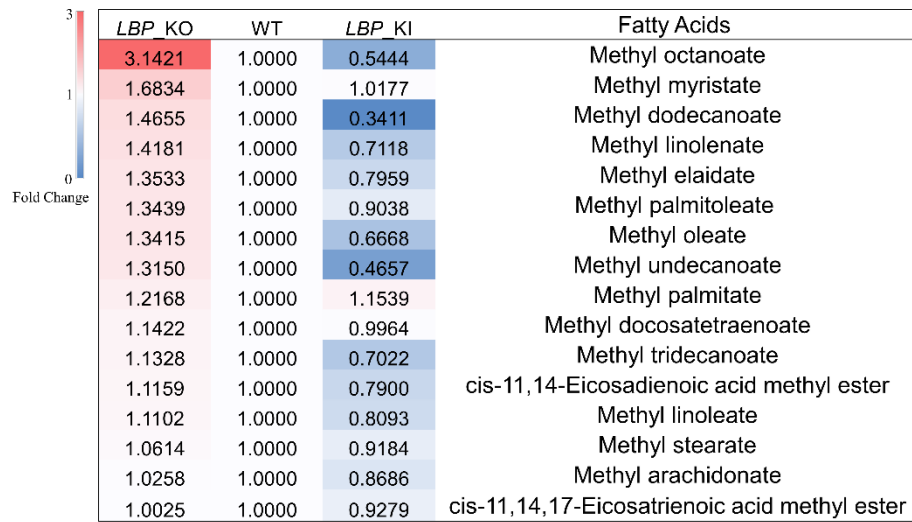
Supplementary Figure S6 C/EBP β may induce transcription activation of *SCD* by binding to *SCD* promoter

A: Potential motif logos for TF C/EBP β predicted using JASPAR (<https://jaspar.genereg.net/>). B: Top 10 potential binding sites of C/EBP β in *SCD* promoter region predicted using JASPAR (<https://jaspar.genereg.net/>).

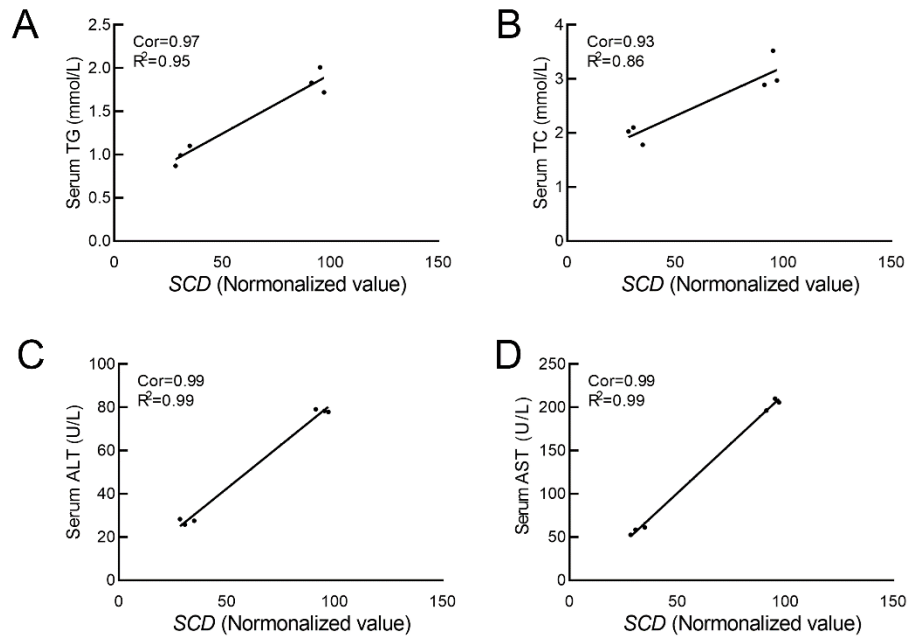


Supplementary Figure S7 siSCD significantly reduces PA-induced lipid accumulation in hepatocytes

A, B: Validation of *SCD* knockdown in BRL-3A hepatocytes by western blot analysis (A) and RT-qPCR (B), respectively. $n=3$ /group. C: Images of Oil-red O staining of *SCD*-knockdown BRL-3A hepatocytes and controls stimulated with PA or BSA ($n=3$ /group). Scale bar, 100 μ m. D: Hepatic TG levels after different processing in BRL-3A hepatocytes ($n=3$ /group). Student's *t*-test or one-way ANOVA was performed for data analysis as appropriate. **: $P<0.01$; ***: $P<0.001$. Data are shown as mean \pm SD.

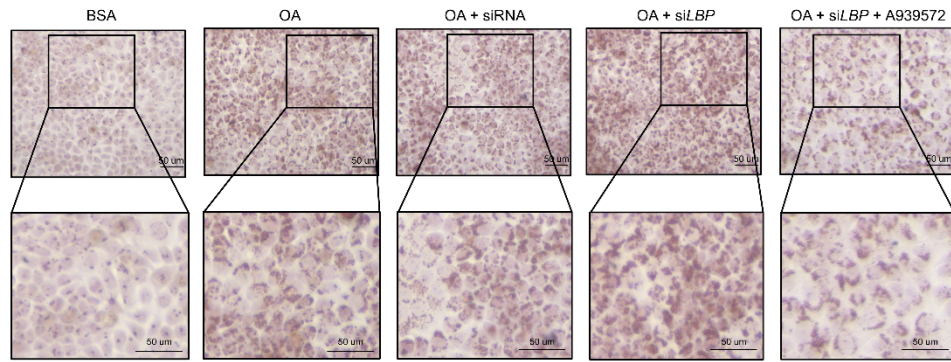


Supplementary Figure S8 Metabolomic analysis reveals increased liver fatty acid content induced by *LBP* knockout in HFD-fed rats



Supplementary Figure S9 Correlation between *SCD* expression and NAFLD parameters in *LBP*^{-/-} rats

A–D: Correlation between *SCD* expression in RNA-Seq data and serum TG (A), TC (B), ALT (C), and AST (D) contents in *LBP*^{-/-} individuals (*n*=3/group).



Supplementary Figure S10 Images of Oil-red O staining of HepG2 hepatocytes in indicated groups ($n=3$ /group)

Scale bar, 50 μm.

Supplementary Table S1 Primers for RT-qPCR

Primer	Sequence 5'→3'
Rat <i>IL6</i>	F: GTTGCCTTCTTGGGACTG R: ACTGGTCTGTTGTGGGTG
Rat <i>TNF-α</i>	F: GCTCCCTCTCATCAGTTCCA R: GCTTGGTGGTTTGCTACGAC
Rat <i>FASN</i>	F: GGAGGTGGTGATAGCCGGTAT R: TGGGTAATCCATAGAGCCCAG
Rat <i>SREBP1c</i>	F: GGAGCCATGGATTGCACATT R: AGGAAGGCTTCCAGAGAGGA
Rat <i>LBP</i>	F: TCAGGCCTTCAACATAGCCA R: TTGGAGTCAGGCGGTAACAT
Rat <i>SCD</i>	F: CCAAGAACCTCCTGGGCTAA R: AACTGCCCTTGAGGTAGGTC
Rat <i>C/EBPβ</i>	F: CGACTTCCTTTCCGACCTCT R: GAGGCTCACGTAACCGTAGT
Rat <i>β-actin</i>	F: CACCATGTACCCAGGCATTG R: CCTGCTTGCTGATCCACATC
Mouse <i>PPARα</i>	F: TATTCGGCTGAAGCTGGTGTAC R: CTGGCATTGTTCGGTTCT
Mouse <i>SLC25A20</i>	F: GACGAGCCGAAACCCATCAG R: AGTCGGACCTTGACCGTGT
Mouse <i>FATP1</i>	F: CTGGGACTTCCGTGGACCT R: TCTTGCAGACGATACGCAGAA
Mouse <i>MLYCD</i>	F: GCACGTCCGGGAAATGAAC R: GCCTCACACTCGCTGATCTT
Mouse <i>HADHA</i>	F: TGCATTTGCCGCAGCTTTAC R: GTTGGCCCAGATTCGTTCA
Mouse <i>HADHB</i>	F: TCGGGTTTGTTCATCGGA R: GGCCAGAAGCTATCAGACCAA
Mouse <i>ACADM</i>	F: AACACAACACTCGAAAGCGG R: TTCTGCTGTTCCGTCAACTCA
Mouse <i>DECRI</i>	F: GATCCGGGTCTCAGAGGTTT R: ATCAGGTGGTAGCATAGGCTT
Mouse <i>β-actin</i>	F: GTGACGTTGACATCCGTAAGA R: GCCGACTCATCGTACTCC

Supplementary Table S2 Primers for luciferase reporter assay

Primer	Sequence 5'→3'
Site 1	F: AAGAGAAATAGAATGAAAATAT R: GCATGCGCCACCACACTTAGCTA
Site 2	F: CACAGAGAGGCTTACAGAAAAC R: GACTCCGGCCGCACACACAGG
Site 3	F: GGGTCAGAGCATCTCAGGGACC R: TTCACCCAGCAGCAGGCGAAAG

Supplementary Table S3 Top 10 up- and down-regulated genes based on RNA-Seq of *LBP*^{-/-}ND and WT_{ND} livers (ranked by *P*-value)

Gene	log ₂ (fold-change)	<i>P</i> -value	<i>P</i> adj	Related function
Up-regulated				
<i>KATI4</i>	1.62	1.03E-05	2.83E-02	Component of histone acetyltransferase activity on histones H3 and H4; Weakening of histone acetyltransferase activity toward histone H4
<i>GTF2I</i>	3.80	1.34E-05	2.83E-02	RNA polymerase II transcription initiation and promoter of Akt signaling; DNA-binding transcription factor activity
<i>ITIH4</i>	9.19	1.65E-05	2.83E-02	Elevated platelet cytosolic Ca ²⁺ ; Serine-type endopeptidase inhibitor activity and endopeptidase inhibitor activity
<i>RAPGEF4</i>	3.15	3.42E-05	4.01E-02	Cytoskeletal signaling and elevated platelet cytosolic Ca ²⁺ ; Guanyl-nucleotide exchange factor activity and small GTPase binding
<i>GORASP2</i>	3.82	5.01E-05	4.60E-02	Gene silencing by RNA and cell cycle, mitotic
<i>RPS6KA4</i>	2.09	6.38E-05	4.88E-02	Interferon pathway; Transfer protein tyrosine kinase activity; Gene activation by histone phosphorylation and regulation of inflammatory genes
<i>MATR3</i>	3.63	6.77E-05	4.88E-02	Related to nucleic acid binding and nucleotide binding
<i>CYP2C7</i>	1.55	6.82E-05	4.88E-02	Response to ethanol, lipopolysaccharide
<i>KIF16B</i>	1.72	7.46E-05	4.88E-02	Elevated platelet cytosolic Ca ²⁺ and Golgi-to-ER retrograde transport
<i>ARHGAP29</i>	2.88	9.91E-05	5.10E-02	GTPase activator activity and PDZ domain binding; Dampening of ROCK and MYH9 activities in endothelial cells
Down-regulated				
<i>VDAC2</i>	-5.18	1.54E-05	2.83E-02	Metabolite diffusion across mitochondrial outer membrane; Cytoskeletal signaling and deubiquitylation;
<i>RF00002</i>	-6.66	7.22E-05	4.88E-02	/
<i>LOC259244</i>	-5.07	1.52E-04	5.48E-02	Predicted to enable odorant binding activity and active in extracellular space
<i>PFN1</i>	-6.30	1.66E-04	5.76E-02	RNA binding and actin binding
<i>AC120071.1</i>	-7.96	1.68E-	5.76E-	/

		04	02	
<i>UBE2C</i>	-1.95	2.80E-04	8.16E-02	APC-Cdc20 mediated degradation of Nek2A and cell cycle; Ligase activity and ubiquitin protein ligase binding
<i>TARS</i>	-2.20	3.55E-04	9.73E-02	Catalyze the aminoacylation of tRNA; Metabolism of proteins
<i>CHTOP</i>	-1.59	1.13E-03	1.80E-01	Transport of mature transcript to cytoplasm and gene expression; RNA binding
<i>LOC100910979</i>	-1.78	1.79E-03	1.99E-01	/
<i>PACSIN3</i>	-2.92	1.85E-03	1.99E-01	Clathrin-mediated endocytosis and vesicle-mediated transport; Lipid binding and cytoskeletal protein binding

Supplementary Table S4 Top 10 up- and down-regulated genes based on RNA-Seq of *LBP*^{-/-} HFD and WT_HFD livers (ranked by *P*-value)

Gene	log ₂ (fold-change)	<i>P</i> -value	<i>P</i> _{adj}	Related function
Up-regulated				
<i>ATP5MG</i>	2.15	3.95E-81	6.93E-77	Organelle biogenesis and maintenance and transcriptional activation of mitochondrial biogenesis
<i>NDUFA2</i>	2.31	1.71E-79	1.50E-75	ATP synthesis by chemiosmotic coupling; Complex I biogenesis; NADH dehydrogenase (ubiquinone) activity
<i>COX8A</i>	2.16	7.83E-68	4.58E-64	Cytochrome-c oxidase activity; ATP synthesis by chemiosmotic coupling
<i>TIMM13</i>	2.22	3.76E-67	1.65E-63	Related to peroxisomal lipid metabolism
<i>MT-ND3</i>	2.28	2.38E-62	5.23E-59	ATP synthesis by chemiosmotic coupling; Metabolism; NADH dehydrogenase (ubiquinone) activity
<i>NDUFB2</i>	2.20	6.58E-52	6.41E-49	ATP synthesis by chemiosmotic coupling; Complex I biogenesis; NADH dehydrogenase (ubiquinone) activity
<i>HINT1</i>	2.04	2.25E-42	1.41E-39	Nucleotide binding and protein kinase C binding; Modulation of proteasomal degradation of target proteins
<i>BOLA1</i>	2.22	3.85E-42	2.33E-39	Protect cells against oxidative stress
<i>ATP5MF</i>	2.12	3.13E-36	1.37E-33	Organelle biogenesis and maintenance and transcriptional activation of mitochondrial biogenesis
<i>COPS9</i>	2.06	3.58E-35	1.50E-32	Involved in cellular and developmental processes; Regulator of ubiquitin (UBI)

Down-regulated				conjugation
<i>FLT1</i>	-2.29	8.54E-63	2.14E-59	PI3K-Akt signaling pathway and VEGF pathway; Activation of MAP kinase and AKT1 signaling pathway
<i>DCHS1</i>	-2.72	1.26E-54	1.69E-51	ERK signaling; Calcium-dependent cell-adhesion protein
<i>BMPR2</i>	-2.80	2.96E-52	3.17E-49	Akt signaling; Transferase activity and protein tyrosine kinase activity
<i>DGKH</i>	-4.04	6.70E-45	4.89E-42	GPCR downstream signaling; Response to elevated platelet cytosolic Ca ²⁺ ; NAD ⁺ kinase activity
<i>ERG</i>	-2.26	4.92E-39	2.54E-36	Chromatin regulation/Acetylation; Transcriptional regulation through recruitment of SETDB1 histone methyltransferase and modification
<i>AKAP2</i>	-3.29	2.16E-36	9.70E-34	GPER1 signaling and VEGFA-VEGFR2 signaling pathway
<i>SOGAI</i>	-3.89	6.51E-35	2.65E-32	Insulin receptor signaling pathway; Negative regulation of gluconeogenesis; Regulation of autophagy
<i>HEG1</i>	-2.92	4.05E-33	1.56E-30	Calcium ion binding activity; Negative regulation of Rho protein signal transduction
<i>CCDC88A</i>	-2.60	4.10E-33	1.56E-30	Bifunctional modulator of guanine nucleotide-binding proteins; Regulation of DNA replication and cell proliferation; AKT-mTOR signaling pathway
<i>ZEB2</i>	-2.44	1.41E-32	5.16E-30	Nucleic acid binding and phosphatase regulator activity; Repression of E-cadherin transcription

Supplementary Table S5 Top 10 hypo- and hyper-acetylated peaks identified by ChIP-Seq in *LBP*^{-/-}ND rats (ranked by *P*-value)

Chr.	Position (Start-End)	log₂ (fold-change)	<i>P</i>-value	<i>P</i>_{adj}	Regulation
Hypoacetylated peaks					
1	99044194-99047503	-12.58	4.30E-23	1.15E-18	DR
17	19194861-19202125	-1.41	2.11E-21	2.81E-17	DR
1	99051650-99052303	-12.14	1.90E-20	1.69E-16	DR
6	95378485-95389760	-1.69	1.04E-15	6.96E-12	DR
6	43207373-43211188	-2.21	3.07E-13	1.63E-09	DR
1	177006246-177010630	-1.89	2.54E-12	9.75E-09	DR
8	75555207-75575491	-1.72	2.63E-12	9.75E-09	DR
1	204616297-204632772	-1.34	2.93E-12	9.75E-09	DR
6	92596092-92601011	-2.76	4.43E-11	1.18E-07	DR
3	127393649-127395538	-3.81	8.55E-11	2.02E-07	DR
Hyperacetylated peaks					
17	69452402-69462956	1.77	6.79E-09	7.51E-06	UR
5	77246433-77247383	1.91	1.86E-08	1.42E-05	UR
5	77569030-77573406	1.74	7.25E-08	4.20E-05	UR
8	38142909-38155473	1.51	8.02E-08	4.55E-05	UR
4	168207524-168212107	1.98	5.57E-07	2.39E-04	UR
2	243715676-243721043	1.31	1.72E-06	5.67E-04	UR
8	41762881-41770021	2.33	1.96E-06	6.08E-04	UR
2	243506520-243532810	1.28	3.83E-06	1.08E-03	UR
2	243689941-243696236	2.00	4.93E-06	1.27E-03	UR
9	49566950-49567828	1.73	5.27E-06	1.33E-03	UR

Supplementary Table S6 Top 10 hypo- and hyper-acetylated peaks identified by ChIP-Seq in *LBP*^{-/-} HFD rats (ranked by *P*-value)

Chr.	Position (Start-End)	log₂ (Fold Change)	<i>P</i>-value	<i>P</i>adj	Regulation
Hypoacetylated peaks					
4	152884936-152888430	-2.69	2.27E-46	1.27E-41	DR
8	41650552-41653034	-11.37	1.68E-25	4.70E-21	DR
1	213242398-213243753	-6.53	1.66E-22	3.08E-18	DR
8	41646554-41649230	-10.52	1.27E-21	1.77E-17	DR
1	259165910-259167705	-11.40	7.89E-19	7.33E-15	DR
8	41639540-41641028	-7.53	1.73E-18	1.13E-14	DR
9	73995039-73997415	-11.40	1.82E-18	1.13E-14	DR
2	263802363-263803642	-10.82	5.36E-18	2.99E-14	DR
3	154788368-154791693	-10.41	5.27E-16	2.45E-12	DR
8	112634080-112641325	-1.89	1.09E-15	4.66E-12	DR
Hyperacetylated peaks					
7	124987182-124992573	7.79	1.83E-19	2.04E-15	UR
18	55379481-55382440	2.73	1.63E-18	1.13E-14	UR
9	96760981-96764971	2.63	2.34E-17	1.19E-13	UR
5	23427224-23428654	10.25	1.55E-15	6.18E-12	UR
11	88948329-88949962	10.17	4.22E-15	1.47E-11	UR
5	104362635-104363698	9.99	1.56E-14	4.58E-11	UR
2	232585919-232587723	6.12	7.43E-14	1.97E-10	UR
3	154812697-154814599	6.29	1.33E-12	2.86E-09	UR
19	27855994-27856351	9.69	3.83E-12	7.36E-09	UR
18	55373240-55374482	2.85	2.31E-11	3.68E-08	UR

Supplementary Table S7 Fatty acid oxidation (FAO)-related genes indicated in this study

Gene	Symbol	FAO-related function	Correlation with FAO activity
<i>PPARα</i>	Peroxisome proliferator-activated receptor α	<i>PPARα</i> , as a regulator, is widely reported to positively control expression of genes involved in liver peroxisomal FAO.	Positive
<i>SLC25A20</i>	Solute carrier family 25 member 20	<i>SLC25A20</i> encoded protein mediates transport of acylcarnitines into mitochondrial matrix for oxidation by mitochondrial FAO pathway.	Positive
<i>FATP1</i>	Fatty acid transport protein 1	<i>FATP1</i> encoded protein is evolutionarily conserved and localizes to plasma membrane to enhance transportation of fatty acids (FAs), involving in FAO.	Positive
<i>MLYCD</i>	Malonyl-CoA decarboxylase	Product of <i>MLYCD</i> catalyzes breakdown of malonyl-CoA to acetyl-CoA and carbon dioxide and inhibits transport of fatty acyl CoAs into mitochondria, increasing rate of FAO.	Positive
<i>HADHA</i>	Hydroxyacyl-CoA dehydrogenase trifunctional multienzyme complex subunit alpha	<i>HADHA</i> encodes alpha subunit of mitochondrial trifunctional protein, which catalyzes the last three steps of mitochondrial beta-oxidation of long chain FAs.	Positive
<i>HADHB</i>	Hydroxyacyl-CoA dehydrogenase trifunctional multienzyme complex subunit beta	<i>HADHB</i> encodes beta subunit of mitochondrial trifunctional protein, which catalyzes the last three steps of mitochondrial beta-oxidation of long chain FAs.	Positive
<i>ACADM</i>	Acyl-CoA dehydrogenase medium chain	<i>ACADM</i> encodes medium-chain specific (C4 to C12 straight chain) acyl-Coenzyme A dehydrogenase, which catalyzes initial step of mitochondrial FA beta-oxidation pathway.	Positive
<i>DECRI</i>	Mitochondrial 2,4-dienoyl-CoA reductase 1	<i>DECRI</i> encodes accessory enzyme, which participates in beta-oxidation and metabolism of unsaturated fatty enoyl-CoA esters.	Positive